Published in final edited form as:
Neuroscience. 2011 April 28; 180: 111–121. doi:10.1016/j.neuroscience.2011.02.023.

PREPROGLUCAGON NEURONS PROJECT WIDELY TO AUTONOMIC CONTROL AREAS IN THE MOUSE BRAIN

Ida J Llewellyn-Smith[a], **Frank Reimann**[b], **Fiona M Gribble**[b], and **Stefan Trapp**[c]

[a]Cardiovascular Medicine, Physiology and Centre for Neuroscience, Flinders University, Bedford Park SA 5042, Australia

[b]Cambridge Institute for Medical Research; Wellcome Trust/MRC Building, Addenbrooke's Hospital, Hills Road, Cambridge, CB2 2XY, UK

[c]Department of Surgery and Cancer & Biophysics Section; South Kensington Campus, Imperial College, London, SW7 2AZ, UK

Abstract

Glucagon-like peptide 1 (GLP-1) and its analogue exendin-4 inhibit food intake, reduce blood glucose levels and increase blood pressure and heart rate by acting on GLP-1 receptors in many brain regions. Within the central nervous system, GLP-1 is produced only by preproglucagon (PPG) neurons. We suggest that PPG neurons mediate the central effects of GLP-1 by modulating sympathetic and vagal outflow. We therefore analysed the projections of PPG neurons to brain sites involved in autonomic control. In transgenic mice expressing YFP under the control of the PPG promoter, we assessed YFP-immunoreactive innervation using an anti-GFP antiserum and avidin-biotin-peroxidase.

PPG neurons were intensely YFP-immunoreactive and axons could be easily discriminated from dendrites. YFP-immunoreactive cell bodies occurred primarily within the caudal nucleus tractus solitarius (NTS) with additional somata ventral to the hypoglossal nucleus, in raphé obscurus and in the intermediate reticular nucleus. The caudal NTS contained a dense network of dendrites, some of which extended into the area postrema. Immunoreactive axons were widespread throughout NTS, dorsal vagal nucleus and reticular nucleus with few in the hypoglossal nucleus and pyramids. The dorsomedial and paraventricular hypothalamic nuclei, ventrolateral periaqueductal grey and thalamic paraventricular nucleus exhibited heavy innervation. The area postrema, rostral ventrolateral medulla, pontine central grey, locus coeruleus/Barrington's nucleus, arcuate nucleus and the vascular organ of the lamina terminalis were moderately innervated. Only a few axons occurred in the amygdala and subfornical organ.

Our results demonstrate that PPG neurons innervate primarily brain regions involved in autonomic control. Thus, central PPG neurons are ideally situated to modulate sympathetic and parasympathetic outflow through input at a variety of central sites. Our data also highlight that immunohistochemistry improves detection of neurons expressing YFP. Hence, animals in which

Correspondence to: Dr Stefan Trapp, Huxley Building, Room 732, Biophysics Section, South Kensington Campus, Imperial College London, London, SW7 2AZ, phone: ++44 (0)20 7594 7912, Fax: ++44 (0)20 7594 7628, s.trapp@imperial.ac.uk.

Europe PMC Funders Author Manuscripts

specific populations of neurons have been genetically-modified to express fluorescent proteins are likely to prove ideal for anatomical studies.

Keywords

Glucagon-like peptide 1; Area postrema; Dorsal vagal complex; Hypothalamus; Green fluorescent protein; Immunohistochemistry

INTRODUCTION

Glucagon-like peptide 1 (GLP-1) is an incretin that facilitates absorption of nutrients and decreases appetite (Holst, 2007). GLP-1 is released into the bloodstream postprandially from L-cells in the small intestine and colon. It acts both on peripheral receptors, e.g., in pancreas, and within the central nervous system (CNS). Receptors for GLP-1 are found in many brain regions (Shughrue et al., 1996, Merchenthaler et al., 1999). Both peripheral and central application of GLP-1 inhibits food intake and reduces blood glucose levels (Kreymann et al., 1987, Tang-Christensen et al., 1996, Turton et al., 1996, Flint et al., 1998, Abbott et al., 2005, Sandoval et al., 2008). Activation of central GLP-1 receptors also increases blood pressure and heart rate (Cabou et al., 2008).

GLP-1 in the bloodstream is rapidly degraded by dipeptidyl peptidase-4 (DPP-4) into an inactive N-terminally truncated form (Kieffer et al., 1995, Holst and Deacon, 2005) and it is unclear whether GLP-1 can cross the blood brain barrier (Orskov et al., 1996, Kastin et al., 2002). Hence, it is unlikely that gut-derived GLP-1 could reach the majority of GLP-1 receptors within the CNS. Peripheral GLP-1 might only reach receptors in circumventricular organs, i.e., the area postrema (AP), the subfornical organ (SFO) and the vascular organ of the lamina terminalis (OVLT).

Preproglucagon (PPG) neurons, which are primarily located in the lower brainstem, are the only recognised endogenous source of GLP-1 within the CNS. The largest population of GLP-1 immunoreactive somata has been found in the caudal nucleus tractus solitarius (NTS) and there are also some cell bodies in the dorsomedial part of the medullary reticular nucleus (Jin et al., 1988, Larsen et al., 1997). mRNA encoding PPG occurs in these same areas (Merchenthaler et al., 1999). The dorsomedial and paraventricular nuclei of the hypothalamus have been reported to contain the densest GLP-1-immunoreactive innervation with the least innervation in the cortex and hindbrain (Jin et al., 1988, Vrang et al., 2007, Tauchi et al., 2008).

The distribution of GLP-1 axons described to date is somewhat surprising given recent evidence highlighting the importance of hindbrain GLP-1 receptors for physiological function (Wan et al., 2007a, Wan et al., 2007b, Hayes et al., 2008, Hayes et al., 2009, Holmes et al., 2009, Williams et al., 2009; see also Trapp and Hisadome, 2010 for review). Until recently, direct functional characterisation of PPG neurons has been hampered by the difficulty in identifying these cells. We have now overcome this problem by producing a transgenic mouse that expresses yellow fluorescent protein (YFP) under control of the PPG promotor (Reimann et al., 2008). The first functional study of these neurons at the cellular

Europe PMC Funders Author Manuscripts

level revealed that the PPG neurons in the NTS do not have functional GLP-1 receptors (Hisadome et al., 2010).

These recent physiological findings prompted us to revisit the projection pattern of PPG neurons, with particular emphasis on the hindbrain. We used the transgenic YFP-PPG mice in order to take advantage of the strong YFP expression that occurs throughout the cytoplasm of these neurons, including their terminals (Hisadome et al., 2010). For the present study, we used an anti-GFP antiserum and revealed its location with avidin-biotin-peroxidase. Immunohistochemical detection significantly enhanced the native fluorescent signal of the YFP. This improvement allowed us to discriminate unequivocally between axons and dendrites and to reveal new central sites that receive innervation from hindbrain PPG neurons.

EXPERIMENTAL PROCEDURES

These studies were performed on 9 adult male and 8 adult female mGLU-124 Venus YFP mice (Reimann et al., 2008). These will be referred to as YFP-PPG mice in this study. Mice weighed between 25 and 35g and were 12-16 weeks of age. Males were consistently heavier than females of the same age. All animals were bred in-house, were kept on a 12 hour light:dark cycle and had access to food and water *ad libitum*. All experiments were carried out in accordance with the UK Animals (Scientific Procedures) Act, 1986, with appropriate ethical approval.

Mice were anesthetized with halothane and heparinised (500 IU/l). Phosphate-buffered saline was flushed through their vascular systems to remove blood. The mice were then perfused transcardially with 60 ml of 4% formaldehyde in 0.1M phosphate buffer, pH 7.4. Brains were post-fixed intact for 3 days at room temperature on a shaker in the same fixative. After post-fixation, the brains were sent to Flinders for sectioning and immunohistochemical processing.

The brains were trimmed to remove regions rostral to the third ventricle and caudal to the spinomedullary junction. The resulting blocks were infiltrated with 20% and then 30% sucrose and cut transversely at 30μm on a cryostat into 3 series of sections. A matrix was not used to trim the brains so that the dorsoventral tilt of the sections varied among mice. We could not therefore reliably assign Bregma values to the regions in which we observed YFP-PPG neurons or axons and have described the location of immunoreactive structures in relation to common anatomical landmarks.

Immunohistochemistry

YFP-PPG neurons were visualized with a chicken antiserum directed against green fluorescent protein (Catalogue #AB13970, lot #623923; Abcam, Cambridge MA, USA). Titration was used to determine the working concentration. The optimal dilution was identified as that which produced the maximum number of immunoreactive structures with a minimal amount of non-specific staining. More concentrated antiserum was used to optimally visualize axons than for optimally visualizing cell bodies. Tissue that lacked

fluorescent protein-expressing neurons showed no staining after immunoperoxidase processing to reveal GFP.

The cryostat sections were permeabilized for immunostaining by washing 3 × 10 min in 10 mM Tris, 0.9% NaCl, 0.05% thimerosal in 10 mM phosphate buffer, pH 7.4 (TPBS) containing 0.3% Triton X-100. Before incubation in primary antibodies, the sections were exposed for at least 30 min to TPBS-Triton containing 10% normal horse serum (NHS) to block non-specific binding of the primary antibodies. The anti-GFP was diluted with TPBS-Triton containing 10% NHS; secondary antibodies, with TPBS-Triton containing 1% NHS; and; the avidin complexes, with TPBS-Triton. Sections were washed 3 × 10 min in TPBS after each incubation and all incubations and washes were done at room temperature on a shaker.

Immunohistochemical detection of YFP

Immunoperoxidase labelling: After permeabilization with TBS-Triton and blocking with 10% NHS-TBS-Triton, the sections were transferred into a 1:20,000 or 1:50,000 dilution of chicken anti-GFP. After 3-5 days in primary antiserum, the sections were incubated overnight in biotinylated donkey anti-chicken IgY (Catalogue #703-065-155; Jackson ImmunoResearch, West Grove PA) diluted 1:500, followed by a 4-6 hr incubation in ExtrAvidin-horseradish peroxidase diluted 1:1,500 (Catalogue # E-2886; Sigma-Aldrich, St Louis MO, USA). Finally, YFP-immunoreactive neurons were visualized with a nickel-intensified diaminobenzidine (DAB) reaction in which peroxide was generated by glucose oxidase (Llewellyn-Smith et al., 2005). After immunoperoxidase staining, sections were mounted in serial order onto chrome alum-gelatine coated slides, dried and dehydrated. Permaslip mounting medium (Alban Scientific, St Louis MO, USA) was used for the application of coverslips.

Immunofluorescent labelling: Fluorescent immunolabelling of YFP-expressing neurons was done with a 1:50,000 dilution of anti-GFP and the same protocol as for peroxidase immunolabelling except that ExtrAvidin-horseradish peroxidase was replaced by a 1:1000 dilution of Cy3-Streptavidin (Amersham Catalogue # PA43001; GE Healthcare Bio-Sciences Pty. Ltd., Rydalmere NSW, Australia). Sections stained for immunofluorescence were mounted in buffered glycerol in serial order, coverslipped, sealed with nail polish to prevent dehydration and stored in the dark at 4°C until examination.

Data Collection and Analysis

Sections stained using the immunoperoxidase procedure were examined with an Olympus BH-2 microscope. We examined sections from the spinomedullary junction to just rostral of the third ventricle. Digital images from these sections were captured using a SPOT RT colour camera and SPOT RT software version 4.6 (Diagnostic Instruments Inc., Sterling Heights, MI, USA).

Sections of medulla and caudal pons stained with the immunofluorescence procedure were examined with an Olympus AX70 epifluorescence microscope. The filters on the microscope unequivocally distinguished between the green fluorescence emitted by YFP

and Cy3 fluorescence without bleed-through (fluorescein filter block: Chroma 31001 NB, excitation wavelength 470-490 nm, dichroic wavelength 505 nm, emission wavelength 515-545 nm; Cy3 filter block: Chroma 31002, excitation wavelength 515-550 nm, dichroic wavelength 565 nm, emission wavelength 575-615 nm). Fluorescent neurons were photographed with an Orca high-resolution cooled CCD digital camera (Hamamatsu, Hamamatsu City, Japan) controlled by IPLab Spectrum software (Scanalytics, Inc., Fairfax, VA, USA).

Digital images of immunoreactive neurons produced with both staining procedures were imported into Adobe PhotoShop for adjustment of sharpness, brightness and contrast and for conversion of colour images to grayscale. This software was also used for the production of montages of micrographs and for the preparation of plates.

RESULTS

YFP-immunoreactive innervation was assessed in 9 adult male and 8 adult female YFP-PPG mice. After both immunoperoxidase and immunofluorescent staining, YFP-immunoreactivity was intense throughout the entire cytoplasm of medullary YFP-PPG neurons and it was easy to distinguish between YFP-immunoreactive axons and YFP-immunoreactive dendrites. Varicose YFP-immunoreactive axons had clearly delineated, heavily immunoreactive varicosities and fine intervaricose segments that were constant in diameter. Dendrites were wider than axons; their diameters decreased from proximal to distal and they had tapering tips.

Detection of YFP by Intrinsic Fluorescence versus Fluorescence Immunohistochemistry

In our first series of experiments, we established that the anti-GFP antiserum used here selectively and reliably detected YFP. Transverse sections of the lower brainstem from YFP-PPG mice were incubated with anti-GFP antiserum and immunoreactivity was revealed with Cy3-streptavidin (Figure 1). As reported previously, PPG neurons in YFP-PPG mice showed strong cytoplasmic YFP fluorescence that could be observed in fixed as well as unfixed tissue (Hisadome et al., 2010). Intrinsic YFP fluorescence and YFP immunofluorescence were co-localised to exactly the same cells in every section examined (Figures 1A and 1A’), thus demonstrating that the GFP antibodies reliably detected YFP. The immunofluorescent signal from individual neurons was consistently stronger than the signal from intrinsic YFP fluorescence (Figures 1B and 1B’). Furthermore, many more YFP-containing axons and dendrites were apparent when sections were viewed with the filter for immunohistochemistry with Cy3 (Figure 1B’) than with the filter for native YFP fluorescence (Figure 1B). These observations show the significantly enhanced sensitivity achieved by detecting YFP with immunohistochemistry rather than by its native fluorescence.

Having demonstrated antibody specificity and enhanced sensitivity with immunohistochemistry, we performed the remainder of the study using immunoperoxidase staining so that the sections showed optimal structural resolution and did not degrade.

Distribution of YFP-Immunoreactive Somata and Dendrites

In general, the distribution of YFP-immunoreactive neurons in YFP-PPG mice was comparable to that reported in previous studies of GLP-1 immunoreactive neurons in rats (Larsen et al., 1997).

YFP-immunoreactive cell bodies were located almost exclusively in the medulla oblongata (Figure 2A). Most of the medullary YFP-immunoreactive somata lay within the caudal NTS near its lateral edge (Figure 2B). This group of YFP-immunoreactive NTS neurons began caudal to the caudal tip of AP and extended to approximately the middle of AP. Further rostral, the NTS contained very few isolated small somata with YFP-immunoreactivity. There was a second substantial population of YFP-immunoreactive cell bodies in the intermediate reticular nucleus (IRT). This group of neurons first appeared approximately at the level of mid-AP (Figure 2C). In most mice, these neurons extended to roughly the level at which the NTS lost contact with the fourth ventricle. In two mice, the YFP-immunoreactive IRT neurons were absent rostral to the rostral edge of AP. In addition, a few YFP-immunoreactive somata were observed along the ventral border of the hypoglossal nucleus and in the raphé obscurus around the level of mid-AP (Figure 2A). Within the medulla, no YFP-immunoreactive cell bodies were found outside these structures.

As well as cell bodies, the caudal NTS contained many YFP-immunoreactive dendrites. Some of these dendrites extended into AP (Figure 2B) and there was a dense collection of dendrites, which extended from the YFP-immunoreactive cell bodies in the lateral NTS and ran towards the central canal following the border between the dorsal vagal and hypoglossal nuclei (Figures 2A and B). Other dendrites were observed along the midline ventral to the central canal between left and right hypoglossal nuclei (Figure 2A), in raphé obscurus and in the IRT (Figures 2A and C).

In the pons, a few YFP-immunoreactive neurons were located in the dorsomedial spinal trigeminal nucleus just lateral to the most rostral region of the NTS. Immunoreactivity for YFP also occurred in rare cell bodies in the superior colliculus and in the ventrolateral periaqueductal gray (PAG). In the piriform cortex, a subset of cells that appeared to be pyramidal neurons showed both YFP-immunoreactivity and YFP fluorescence; these YFP-positive neurons were associated with an array of fine YFP-containing terminals.

Distribution of YFP-Immunoreactive Axons

Varicose and non-varicose YFP-immunoreactive axons occurred in many different brain areas. Varicose fibres occurred primarily in regions involved in autonomic control.

Many varicose and non-varicose YFP-immunoreactive axons were found in the lower brainstem. From the spinomedullary junction through to the rostral edge of AP, the NTS and IRT contained mainly varicose axons interspersed with a few non-varicose fibres. Rostral to AP, the density of varicose axons in the NTS declined. The caudal one-third of AP contained the highest density of varicose YFP-immunoreactive axons (Figure 2B), but lower levels were seen throughout AP. In the region around the middle of AP, there were many varicose axons lateral to the hypoglossal nucleus (Figure 2A). YFP-immunoreactive axons occurred throughout most of raphé pallidus from the region beneath mid-AP to the rostral

end of the nucleus. Varicose axons were also present in the lateral paragigantocellular nucleus and in the rostral ventrolateral medulla (RVLM; Figure 3A). Few varicose axons occurred within raphé obscurus at all levels and there were occasional varicose axons along the ventral surface of the medulla.

In the medulla, non-varicose axons were observed mainly within the ventral part of the medullary reticular nucleus. This collection of non-varicose axons was moderately dense from the ventral white matter at the spinomedullary junction to approximately the level at which the central canal opened into the fourth ventricle (Figure 3A). More rostrally within the medullary reticular nucleus, non-varicose fibres were sparse. In the lateral reticular nucleus, axons were mainly non-varicose.

Rostral to the medulla, there were many YFP-immunoreactive axons in the region of Barrington's nucleus and the locus coeruleus (Figure 3B), whereas few varicose fibres occurred in raphé pallidus and raphé magnus and along the ventral surface. Varicose YFP-positive axons were plentiful in the ventrolateral PAG and the density of axons in this region increased from caudal to rostral. Some varicose YFP-containing axons also occurred in the dorsomedial PAG (Figure 3C). Both varicose and non-varicose fibres travelled dorsoventrally through the lateral pons and ran through the mesencephalic reticular formation. Only a few varicose axons were present in the dorsal raphé nuclei and around the midline. Non-varicose fibres were present in the gigantocellular nucleus.

In the forebrain, some of the hypothalamic nuclei were heavily innervated by YFP-immunoreactive axons. The paraventricular nucleus (PVN) contained a particularly high density of varicose axons (Figure 4A). The dorsomedial hypothalamic nucleus (DMH) was also heavily supplied (Figure 4B), with the density of varicose YFP-positive axons peaking in the region approximately equivalent to Bregma −1.70. The innervation of the arcuate nucleus varied rostrocaudally. There was a moderate supply of axons in the caudal portions of the arcuate (Figures 4B and D). However, the density of innervation declined rostrally so that there were relatively few axons in the most rostral portions of the nucleus. The lateral hypothalamic area (LHA) contained a moderate to low density of varicose YFP-containing axons. Varicose axons were sparse in the ventromedial hypothalamic nucleus (Figure 4B) and even fewer immunoreactive axons occurred in the anterior hypothalamic area. YFP-containing axons in the median eminence were extremely rare.

In the forebrain outside of the hypothalamus, the highest densities of YFP-immunoreactive innervation occurred in the paraventricular nucleus of the thalamus (Figure 4C). Varicose axons in the paraventricular nucleus ran along the surface of the third ventricle near its rostral end and there were beaded axons in the tuberomammillary nucleus and the retromammillary region. Varicose YFP-immunoreactive axons were present around the anterior wall of the third ventricle, including in the OVLT (Figure 4E), but YFP innervation was sparse in the SFO (Figure 4C). A few varicose axons were found in the precommissural nucleus and surrounding area and along the ventral surface. Very few YFP-immunoreactive terminals occurred in the amygdala. Non-varicose and variable numbers of varicose axons travelled dorsoventrally around the midline and a few non-varicose fibers were found in the midline dorsal to the third ventricle. The hippocampus was completely devoid of YFP-

immunoreactive innervation and the only varicose axons in the cortex were the fine axons in the piriform cortex that probably arise from the YFP-immunoreactive pyramidal cells in that region.

The schematic diagrams in Figure 5 provide an overview of the distribution of YFP-immunoreactive cell bodies, varicose axons and non-varicose axons within the brains of YFP-PPG mice from the spinomedullary junction to the rostral edge of the third ventricle.

DISCUSSION

We have performed an immunohistochemical study to determine the distribution of brain GLP-1 neurons and their projections between the spinomedullary junction and the anterior wall of the third ventricle in YFP-PPG mice (Reimann et al., 2008). These mice express YFP specifically and exclusively in cells in which the PPG promoter is active (Reimann et al., 2008; Hisadome et al., 2010); i.e. cells that produce PPG, the precursor for glucagon, as well as GLP-1, GLP-2 and oxyntomodulin (Holst, 2007). Consequently, in these mice, YFP occurs in pancreatic α-cells that produce glucagon, in enteroendocrine L-cells and in populations of central neurons that produce GLP-1 and GLP-2 in equimolar amounts (Reimann et al., 2008). Whilst we cannot categorically exclude transgenic YFP-expression in non-PPG cells, this seems unlikely, as the observed YFP distribution matches previous reports of peripheral and central GLP-1 and glucagon immunoreactivity. Furthermore, single-cell RT-PCR has demonstrated that YFP-expressing cells in the NTS also produce PPG mRNA and thus should synthesize GLP-1 in addition to YFP (Hisadome et al, 2010).

Location of YFP-PPG Cell Bodies in the Mouse Brain

The results of the present study indicate that the distribution of PPG-producing nerve cell bodies in the mouse is very similar to that of neurons with GLP-1 immunoreactivity (Larsen et al., 1997) and neurons expressing PPG mRNA (Merchenthaler et al., 1999) in the rat. Observations in both species show that cell bodies capable of synthesizing GLP-1 occur primarily in the caudal part of the NTS and in the medullary reticular nucleus. Here, we also found a few scattered YFP-immunoreactive cell bodies along the midline ventral to the hypoglossal nucleus and in raphé obscurus. These neurons were not previously described by either Larsen et al. (1997) or Vrang et al. (2007). However, one neuron with PPG mRNA was shown below the hypoglossal nucleus by Merchenthaler et al. (1999) and these authors may have missed the PPG-expressing neurons in raphé obscurus because they are few in number.

In addition to new medullary cell bodies, our improved methodology has conclusively shown that YFP-PPG neurons in the NTS have dendrites that extend into AP, a circumventricular organ with a fenestrated/leaky blood-brain barrier. The YFP-PPG dendrites in AP are unlikely to sense circulating GLP-1 because medullary PPG neurons do not express GLP-1 receptors (Hisadome et al., 2010). Nevertheless, a variety of other humoral factors could access YFP-immunoreactive dendrites in AP because of the leaky blood-brain barrier. It is also possible that AP neurons provide synaptic input to nearby dendrites of YFP-PPG neurons since a variety of different neurochemical types of AP neurons have been shown to form synapses within the AP (e.g., Guan et al., 1994, Guan et

al., 1997, 1999, Guan et al., 2000). Regardless of their AP input, many of the YFP-PPG dendrites also travel through the NTS where they receive synapses from sensory afferents and/or second and higher order NTS neurons, as demonstrated functionally (Hisadome et al., 2010).

YFP-PPG Innervation of the Mouse Brain

The intrinsic YFP fluorescence in YFP-PPG mice is intense enough to identify cell bodies and primary processes, allowing functional studies to be done on *in vitro* brain slices from these transgenic animals (Hisadome et al., 2010). However, we have shown here that in fixed tissue native YFP fluorescence is much ***less*** sensitive than immunohistochemistry for revealing varicose YFP-containing axons. Consequently, our study has provided new insights into the brain regions innervated by PPG-synthesizing central neurons. The data we present here show that YFP-PPG neurons in the mouse send axons to many more brain regions than previously reported for GLP-1 immunoreactive neurons in the rat. Because central GLP-1 actions differ between rats and mice, for example in the dependence of LiCl-induced conditioned taste aversion on GLP-1 receptor activation (Lachey et al., 2005), there may, in fact, be gross differences between the two species in the distribution of central axons containing GLP-1. However, we believe that we have identified new areas of GLP-1 innervation due to the markedly increased sensitivity provided by immunohistochemical detection of neurochemically distinct populations of neurons that have been genetically modified to express GFP or, in this case, a GFP analogue.

Innervation of the Brainstem—Our results show that, in the mouse, the axons of medullary PPG neurons ramify extensively within the lower brainstem, particularly within the dorsal vagal complex, the RVLM, ventrolateral PAG and the region of the mouse brain that contains the Barrington's nucleus and the locus coeruleus. Our findings conflict with the results of an immunohistochemical study that identified very few GLP-1-immunoreactive axons in the brainstem (Jin et al., 1988). This discrepancy could have arisen because many GLP-1 axons may contain insufficient peptide to be detected with immunohistochemistry. In contrast, our data indicate that YFP is intensely expressed in the axons of all YFP-PPG neurons.

Although the distribution of YFP-immunoreactive axons in mice is not consistent with the distribution of GLP-1-immunoreactive axons in rats, the distribution of YFP-PPG axons in the dorsal vagal complex that we have described here does correlate well with the distribution of GLP-1 receptors in this region (Merchenthaler et al, 1999). In particular, we found varicose YFP-immunoreactive axons in regions of the NTS that contain many neurons that express GLP-1 receptors. Whilst some controversy remains about whether GLP-1 can cross the blood-brain barrier (Orskov et al., 1996, Kastin et al., 2002), the available evidence suggests that only GLP-1 released from medullary PPG neurons can access central GLP-1 receptors. Although electron microscopic proof is not available, it now seems highly likely that the functional GLP-1 receptors found on pancreas-projecting dorsal vagal neurons (Wan et al., 2007b, Holmes et al., 2009) receive GLP-1 from neighbouring PPG neurons. Because PPG neurons in the NTS do not express GLP-1 receptors (Hisadome et al., 2010), GLP-1 receptors that normally bind GLP-1 released from the PPG neurons probably mediate the

feeding effects of injections of GLP-1 into the fourth ventricle of decerebrate rats (Hayes et al., 2008). Also for the same reason, the suppression of feeding induced by gastric distension after injection of exendin-9 into the fourth ventricle, cannot be caused by GLP-1 acting on PPG neurons (Hayes et al., 2009).

Within the lower brainstem, one location that peripherally derived GLP-1 might reach is the AP which lacks a blood-brain-barrier. GLP-1 and GLP-1 analogues can reach AP when high concentrations are injected peripherally (Orskov et al., 1996, Yamamoto et al., 2003). However, it is unclear whether endogenous GLP-1 released from enteroendocrine L-cells would also reach this region because GLP-1 is rapidly degraded in the blood stream (Holst, 2007). The AP does express high levels of GLP-1 receptors (Goke et al., 1995, Merchenthaler et al., 1999), which are mostly located on catecholaminergic neurons (Yamamoto et al., 2003). Our results show that YFP-PPG neurons send axons into AP and it is possible that GLP-1 released from these terminals, rather than circulating GLP-1, might activate the receptors in AP. YFP-positive axons are also located in the OVLT and SFO, which are also circumventricular organs, as well as in the hypothalamic arcuate nucleus, another region of the brain suspected to have a leaky blood-brain barrier. Clearly, ultrastructural studies are required to determine whether the PPG-YFP axons make synaptic contact with the neurons expressing GLP-1 receptors in these regions.

YFP-PPG Innervation of the Hypothalamus and Amygdala—In general, the distribution in the forebrain of varicose YFP-immunoreactive axons correlates well with the distribution of GLP-1 receptor mRNA reported previously (Merchenthaler et al., 1999). In particular, neurons expressing GLP-1 receptor mRNA have been identified in the PVN, DMH and arcuate nucleus, where we found moderate to high densities of YFP-immunoreactive axon terminals. There is, however, one significant inconsistency between our anatomical observations and the mRNA data. We found no evidence for a YFP-containing innervation in the hippocampus whereas GLP-1 receptor mRNA has been discovered in the CA2 and CA3 regions of the hippocampus, with highest levels in the most caudal part of CA3 (Merchenthaler et al., 1999). Because our study indicates that all axons arising from neurons that produce PPG should be immunoreactive for YFP, it is very unlikely that the hippocampus is innervated by axons that release GLP-1. Consequently, the source of the GLP-1 that activates these hippocampal GLP-1 receptors needs to be identified. Of course, at present, we cannot exclude that hippocampal neurons only express the mRNA for GLP-1 receptors but do not actually produce GLP-1 receptor protein. There may also be a species difference so that in the rat, but not in the mouse, PPG-synthesizing neurons project to the hippocampus.

In this study, we have assumed that the YFP-immunoreactive axons found throughout the brain originate from the PPG-synthesizing nerve cell bodies that are located in the medulla. In support of our assumption, retrograde tracing in rats has shown that neurons in the lower brainstem project to the paraventricular and dorsomedial hypothalamic nuclei and that some of these projection neurons are GLP-1 immunoreactive (Larsen et al., 1997, Vrang et al., 2007). Although we did find YFP-immunoreactive neurons in the piriform cortex, these neurons are highly unlikely to provide YFP-immunoreactive innervation to central autonomic sites. The YFP-positive cortical neurons have the morphology of pyramidal

neurons, which do not send axons outside their own local region of cortex. Consistent with this suggestion, the YFP-positive cortical neurons described here lay within a region that was innervated by numerous fine, YFP-containing terminals and that was also highly circumscribed. Furthermore, the YFP-immunoreactive cell bodies that we identified in the superior colliculus probably do not supply autonomic areas; their small size suggests that their projections are also likely to be local. Moreover, we have not analysed brain regions more rostral than the anterior wall of the third ventricle or regions caudal to the spinomedullary junction. Hence, we cannot exclude that parts of the CNS not examined in this study contain PPG-producing cell bodies that contribute to the projection pattern observed here. In fact, PPG mRNA has been found in the olfactory bulb of rat (Merchenthaler et al., 1999). The same study also found mRNA for GLP-1 receptors in the thoracic spinal cord but did not detect PPG mRNA.

In conclusion, our results demonstrate that medullary neurons capable of synthesizing GLP-1 innervate primarily brain regions involved in autonomic control. Hence, central PPG neurons are in a prime position to modulate sympathetic and parasympathetic outflow through input at a variety of autonomic locations within the central nervous system.

ACKNOWLEDGMENTS

This work was supported by grants from the Medical Research Council [G0600928], UK to ST and the National Health & Medical Research Council of Australia to ILS (Project Grant 229907, Principal Research Fellowship 229921). FMG and FR are supported by Wellcome Trust Senior Research Fellowships (WT088357 and WT084210). Lee Travis provided expert technical assistance.

LITERATURE CITED

Abbott CR, Monteiro M, Small CJ, Sajedi A, Smith KL, Parkinson JR, Ghatei MA, Bloom SR. The inhibitory effects of peripheral administration of peptide YY (3-36) and glucagon-like peptide-1 on food intake are attenuated by ablation of the vagal-brainstem-hypothalamic pathway. Brain Res. 2005; 1044:127–131. [PubMed: 15862798]

Cabou C, Campistron G, Marsollier N, Leloup C, Cruciani-Guglielmacci C, Penicaud L, Drucker DJ, Magnan C, Burcelin R. Brain glucagon-like peptide-1 regulates arterial blood flow, heart rate, and insulin sensitivity. Diabetes. 2008; 57:2577–2587. [PubMed: 18633100]

Flint A, Raben A, Astrup A, Holst JJ. Glucagon-like peptide 1 promotes satiety and suppresses energy intake in humans. J Clin Invest. 1998; 101:515–520. [PubMed: 9449682]

Franklin, KBJ.; Paxinos, G. The mouse brain in stereotaxic coordinates. Third Edition. Elsevier; London: 2007.

Goke R, Larsen PJ, Mikkelsen JD, Sheikh SP. Distribution of GLP-1 binding sites in the rat brain: evidence that exendin-4 is a ligand of brain GLP-1 binding sites. Eur J Neurosci. 1995; 7:2294–2300. [PubMed: 8563978]

Guan JL, Wang QP, Nakai Y. Electron microscopic observation of delta-opioid receptor-1 in the rat area postrema. Peptides. 1997; 18:1623–1628. [PubMed: 9437725]

Guan JL, Wang QP, Nakai Y. Electron microscopic observation of mu-opioid receptor in the rat area postrema. Peptides. 1999; 20:873–880. [PubMed: 10477089]

Guan JL, Wang QP, Ochiai H, Nakai Y. Synaptic relations of GABAergic neurons in the area postrema. Acta Anat (Basel). 1994; 150:198–204. [PubMed: 7817717]

Guan JL, Wang QP, Shioda S. Observation of the ultrastructure and synaptic relationships of angiotensin II-like immunoreactive neurons in the rat area postrema. Synapse. 2000; 38:231–237. [PubMed: 11020225]

Hayes MR, Bradley L, Grill HJ. Endogenous hindbrain glucagon-like peptide-1 receptor activation contributes to the control of food intake by mediating gastric satiation signaling. Endocrinology. 2009; 150:2654–2659. [PubMed: 19264875]

Hayes MR, Skibicka KP, Grill HJ. Caudal brainstem processing is sufficient for behavioral, sympathetic, and parasympathetic responses driven by peripheral and hindbrain glucagon-like-peptide-1 receptor stimulation. Endocrinology. 2008; 149:4059–4068. [PubMed: 18420740]

Hisadome K, Reimann F, Gribble FM, Trapp S. Leptin directly depolarizes preproglucagon neurons in the nucleus tractus solitarius: electrical properties of glucagon-like Peptide 1 neurons. Diabetes. 2010; 59:1890–1898. [PubMed: 20522593]

Holmes GM, Browning KN, Tong M, Qualls-Creekmore E, Travagli RA. Vagally mediated effects of glucagon-like peptide 1: in vitro and in vivo gastric actions. J Physiol. 2009; 587:4749–4759. [PubMed: 19675064]

Holst JJ. The physiology of glucagon-like peptide 1. Physiol Rev. 2007; 87:1409–1439. [PubMed: 17928588]

Holst JJ, Deacon CF. Glucagon-like peptide-1 mediates the therapeutic actions of DPP-IV inhibitors. Diabetologia. 2005; 48:612–615. [PubMed: 15759106]

Jin SL, Han VK, Simmons JG, Towle AC, Lauder JM, Lund PK. Distribution of glucagonlike peptide I (GLP-I), glucagon, and glicentin in the rat brain: an immunocytochemical study. J Comp Neurol. 1988; 271:519–532. [PubMed: 3385016]

Kastin AJ, Akerstrom V, Pan W. Interactions of glucagon-like peptide-1 (GLP-1) with the blood-brain barrier. J Mol Neurosci. 2002; 18:7–14. [PubMed: 11931352]

Kieffer TJ, McIntosh CH, Pederson RA. Degradation of glucose-dependent insulinotropic polypeptide and truncated glucagon-like peptide 1 in vitro and in vivo by dipeptidyl peptidase IV. Endocrinology. 1995; 136:3585–3596. [PubMed: 7628397]

Kreymann B, Williams G, Ghatei MA, Bloom SR. Glucagon-like peptide-1 7-36: a physiological incretin in man. Lancet. 1987; 2:1300–1304. [PubMed: 2890903]

Lachey JL, D'Alessio DA, Rinaman L, Elmquist JK, Drucker DJ, Seeley RJ. The role of central glucagon-like peptide-1 in mediating the effects of visceral illness: differential effects in rats and mice. Endocrinology. 2005; 146:458–462. [PubMed: 15459118]

Larsen PJ, Tang-Christensen M, Holst JJ, Orskov C. Distribution of glucagon-like peptide-1 and other preproglucagon-derived peptides in the rat hypothalamus and brainstem. Neuroscience. 1997; 77:257–270. [PubMed: 9044391]

Llewellyn-Smith IJ, Dicarlo SE, Collins HL, Keast JR. Enkephalin-immunoreactive interneurons extensively innervate sympathetic preganglionic neurons regulating the pelvic viscera. J Comp Neurol. 2005; 488:278–289. [PubMed: 15952166]

Merchenthaler I, Lane M, Shughrue P. Distribution of pre-pro-glucagon and glucagon-like peptide-1 receptor messenger RNAs in the rat central nervous system. J Comp Neurol. 1999; 403:261–280. [PubMed: 9886047]

Orskov C, Poulsen SS, Moller M, Holst JJ. Glucagon-like peptide I receptors in the subfornical organ and the area postrema are accessible to circulating glucagon-like peptide I. Diabetes. 1996; 45:832–835. [PubMed: 8635662]

Reimann F, Habib AM, Tolhurst G, Parker HE, Rogers GJ, Gribble FM. Glucose sensing in L cells: a primary cell study. Cell Metab. 2008; 8:532–539. [PubMed: 19041768]

Sandoval DA, Bagnol D, Woods SC, D'Alessio DA, Seeley RJ. Arcuate glucagon-like peptide 1 receptors regulate glucose homeostasis but not food intake. Diabetes. 2008; 57:2046–2054. [PubMed: 18487451]

Shughrue PJ, Lane MV, Merchenthaler I. Glucagon-like peptide-1 receptor (GLP1-R) mRNA in the rat hypothalamus. Endocrinology. 1996; 137:5159–5162. [PubMed: 8895391]

Tang-Christensen M, Larsen PJ, Goke R, Fink-Jensen A, Jessop DS, Moller M, Sheikh SP. Central administration of GLP-1-(7-36) amide inhibits food and water intake in rats. Am J Physiol. 1996; 271:R848–856. [PubMed: 8897973]

Tauchi M, Zhang R, D'Alessio DA, Stern JE, Herman JP. Distribution of glucagon-like peptide-1 immunoreactivity in the hypothalamic paraventricular and supraoptic nuclei. J Chem Neuroanat. 2008; 36:144–149. [PubMed: 18773953]

Trapp S, Hisadome K. Glucagon-like peptide 1 and the brain: Central actions-central sources? Auton Neurosci. 2010

Turton MD, O'Shea D, Gunn I, Beak SA, Edwards CM, Meeran K, Choi SJ, Taylor GM, Heath MM, Lambert PD, Wilding JP, Smith DM, Ghatei MA, Herbert J, Bloom SR. A role for glucagon-like peptide-1 in the central regulation of feeding. Nature. 1996; 379:69–72. [PubMed: 8538742]

Vrang N, Hansen M, Larsen PJ, Tang-Christensen M. Characterization of brainstem preproglucagon projections to the paraventricular and dorsomedial hypothalamic nuclei. Brain Res. 2007; 1149:118–126. [PubMed: 17433266]

Wan S, Browning KN, Travagli RA. Glucagon-like peptide-1 modulates synaptic transmission to identified pancreas-projecting vagal motoneurons. Peptides. 2007a; 28:2184–2191. [PubMed: 17889966]

Wan S, Coleman FH, Travagli RA. Glucagon-like peptide-1 excites pancreas-projecting preganglionic vagal motoneurons. Am J Physiol Gastrointest Liver Physiol. 2007b; 292:G1474–1482. [PubMed: 17322063]

Williams DL, Baskin DG, Schwartz MW. Evidence that intestinal glucagon-like peptide-1 plays a physiological role in satiety. Endocrinology. 2009; 150:1680–1687. [PubMed: 19074583]

Yamamoto H, Kishi T, Lee CE, Choi BJ, Fang H, Hollenberg AN, Drucker DJ, Elmquist JK. Glucagon-like peptide-1-responsive catecholamine neurons in the area postrema link peripheral glucagon-like peptide-1 with central autonomic control sites. J Neurosci. 2003; 23:2939–2946. [PubMed: 12684481]

Europe PMC Funders Author Manuscripts

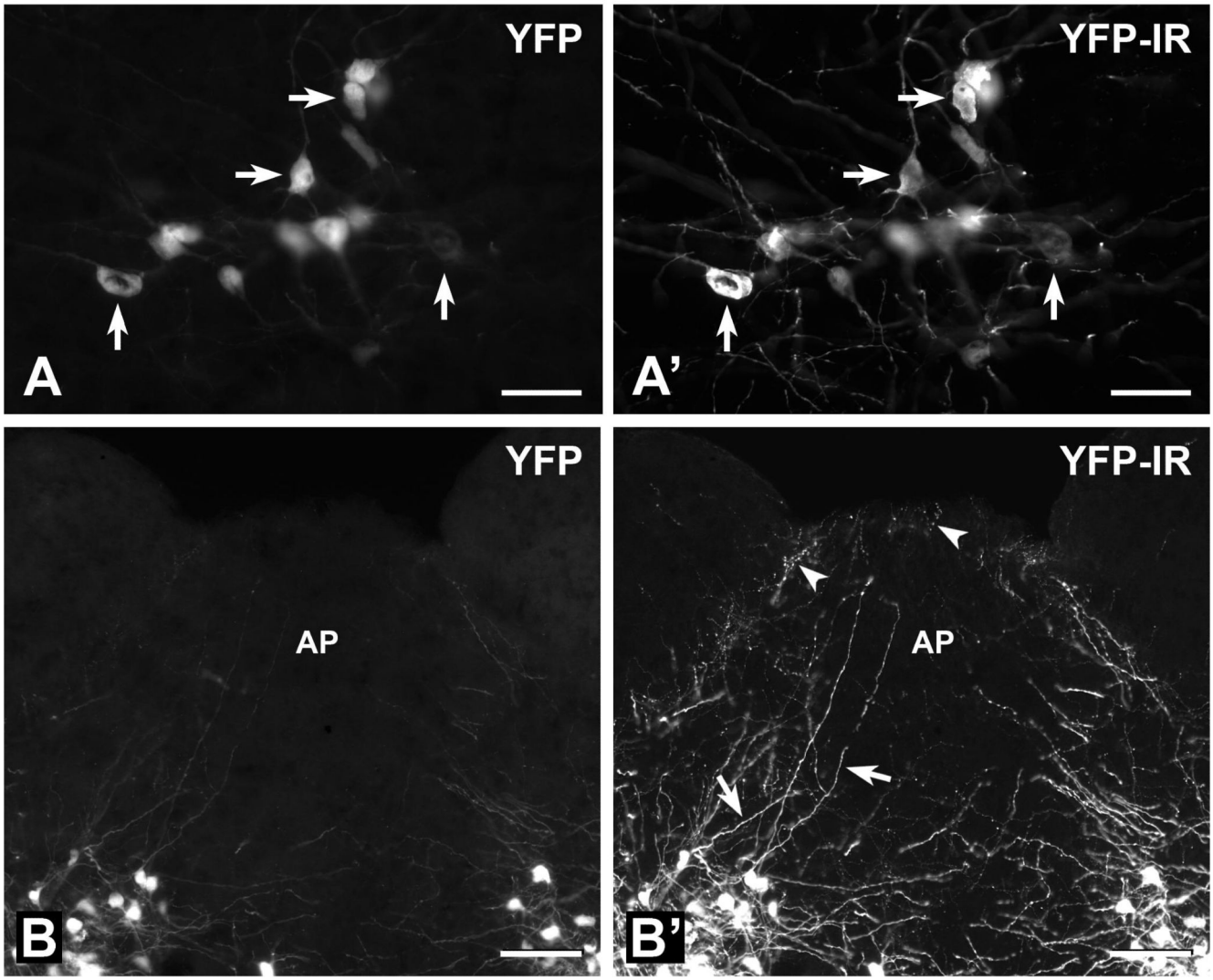

FIGURE 1. Detection of YFP-PPG neurons in the medulla using intrinsic YFP fluorescence versus immunohistochemistry for YFP

YFP-PPG neurons in transverse sections through the medulla that were processed to reveal YFP-immunoreactivity (IR) with an anti-GFP antiserum, biotinylated secondary antibodies and Cy3-streptavidin. **A**, Fourteen YFP-expressing somata in the intermediate reticular nucleus at the level of the rostral area postrema (AP) that were viewed with the filter combination for the intrinsic fluorescence of YFP. Arrows indicate four cell bodies with fluorescent signals that vary from faint to intense. **A'**, The same 14 YFP-containing somata viewed with the filter combination for immunofluorescent detection of YFP with Cy3-streptavidin. A comparison of A and A' shows that all of the YFP-containing cell bodies appear in both micrographs. However, many more YFP-containing axons and dendrites are detected by their YFP-immunoreactivity (YFP-IR) than by the fluorescence due to their YFP content. Bars, 50 μm. **B,** YFP-expressing cell bodies in the NTS and YFP-expressing axons and dendrites in the caudal AP that were visualized using the filter combination for the intrinsic fluorescence of YFP. **B',** The same field of view viewed using the filter

combination for immunofluorescent detection of YFP with Cy3-streptavidin. The backgrounds of the two micrographs were adjusted to the same grayscale values using Adobe PhotoShop. A comparison of B with B’ shows that many more YFP-containing axons with clearly delineated varicosities (arrowheads in B’) are visualized with immunohistochemistry than with native YFP fluorescence. More dendrites (arrows in B’) are also apparent after immunohistochemical detection of YFP and their decreasing diameters and tapering ends are much better revealed. Bars, 100 μm.

Europe PMC Funders Author Manuscripts

Europe PMC Funders Author Manuscripts

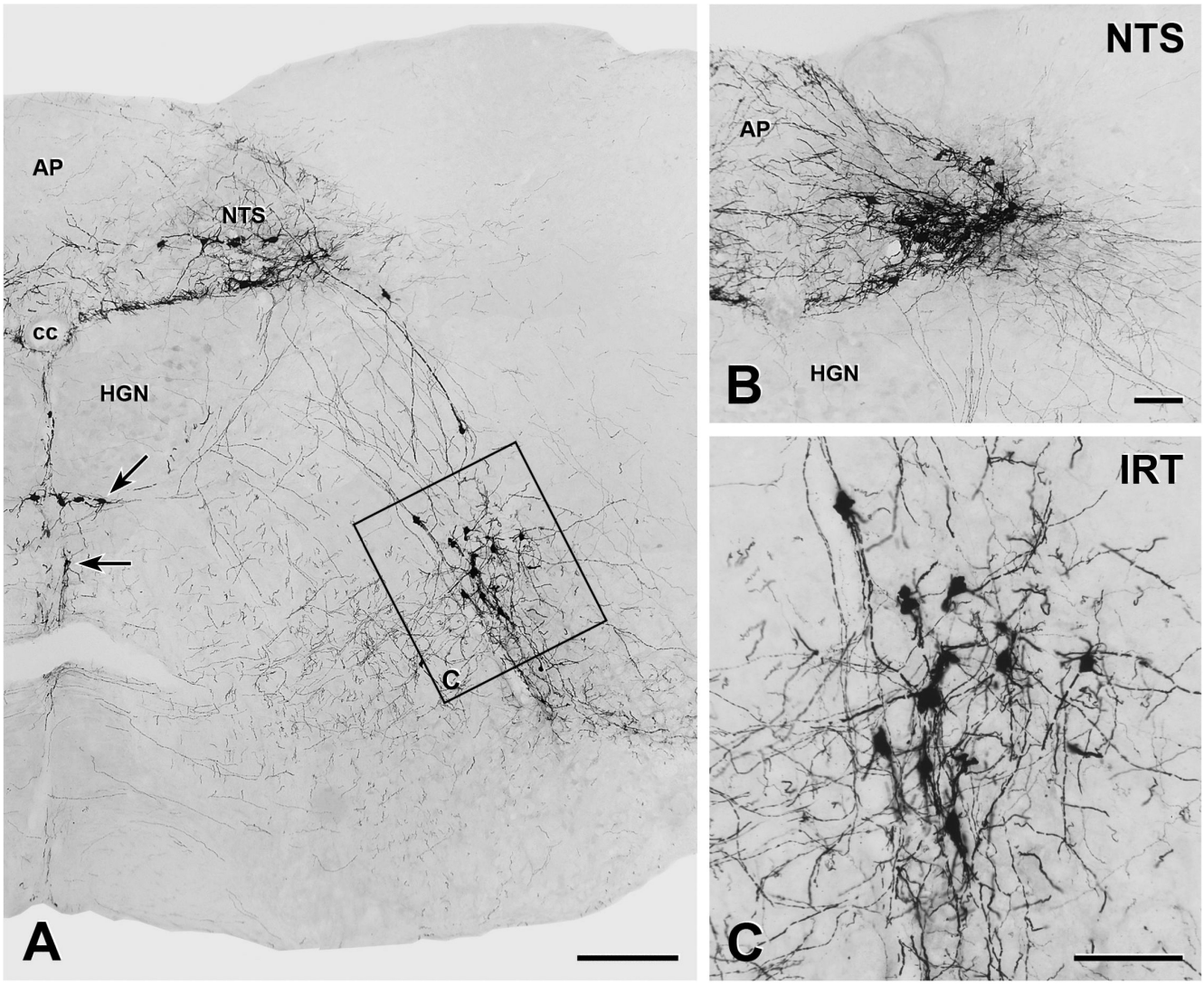

FIGURE 2. Distribution of YFP-immunoreactive neurons in the lower brainstem

YFP-PPG neurons in transverse sections through the medulla were visualised by immuno-peroxidase staining with nickel-intensified diaminobenzidine **A,** Montage of low magnification micrographs showing YFP-immunoreactive cell bodies located in the caudal nucleus tractus solitarius, in the intermediate reticular nucleus, at the ventral border of the hypoglossal nucleus (HGN, arrow) and in raphé obscurus (arrow). There are many YFP-positive dendrites running towards the central canal (cc) along the border between the dorsal vagal nucleus and the HGN. Immunoreactive axons were widespread throughout the NTS, the dorsal vagal nucleus and the reticular nucleus (except for the parvicellular section) but the HGN is virtually devoid of YFP-positive axons. Bar, 250 μm. **B.** The caudal NTS contained YFP-immunoreactive cell bodies and a dense network of dendrites, some of which extended into the area postrema (AP) and the dorsal vagal nucleus. Many axons extend ventrolaterally and some travel along the lateral edge of the HGN. There are also axons that extend into AP and the dorsal vagal nucleus. Bar, 100 μm. **C.** The intermediate reticular

nucleus (IRT) contains another substantial group of YFP-immunoreactive cell bodies. Bar, 100 μm.

Europe PMC Funders Author Manuscripts

Europe PMC Funders Author Manuscripts

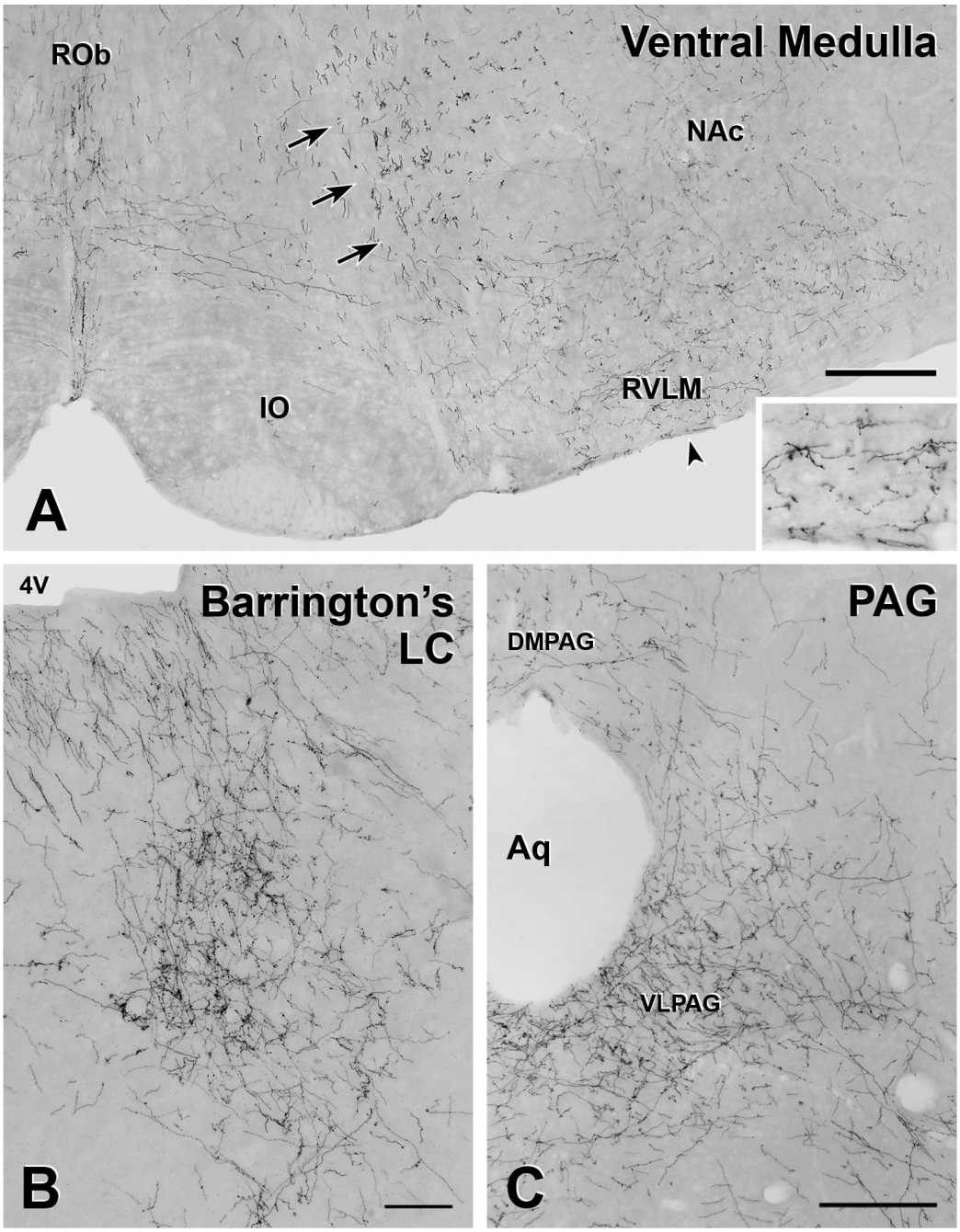

FIGURE 3. YFP-immunoreactive axons in the medulla and midbrain A

The ventral medulla contains both varicose and non-varicose axons. The majority of the axons in the rostral ventrolateral medulla (RVLM) and along the ventral surface of the medulla are varicose. The arrow indicates the location of the inset, which shows these axons at higher magnification. In contrast, in the ventral medullary reticular nucleus, non-varicose axons of passage (arrows) are the most prominent. YFP-positive axons in raphé obscurus are a mixture of varicose and non-varicose whereas YFP-containing axons in raphé pallidus are mainly varicose. Bar, 250 μm. **B**. A dense accumulation of varicose, YFP-immunoreactive

axons occur near the fourth ventricle (4V) in the region of Barrington's nucleus and the locus coeruleus (LC). Bar, 100 μm. **C**. At the level of the aqueduct (Aq) many YFP-immunoreactive axons are present in subregions of the periaqueductal gray (PAG). The ventrolateral PAG (VLPAG) contains a high density of varicose YFP-positive axons, whereas there is a moderate to low density of YFP-containing axons in the dorsomedial PAG (DMPAG). Bar, 250 μm.

Europe PMC Funders Author Manuscripts

Europe PMC Funders Author Manuscripts

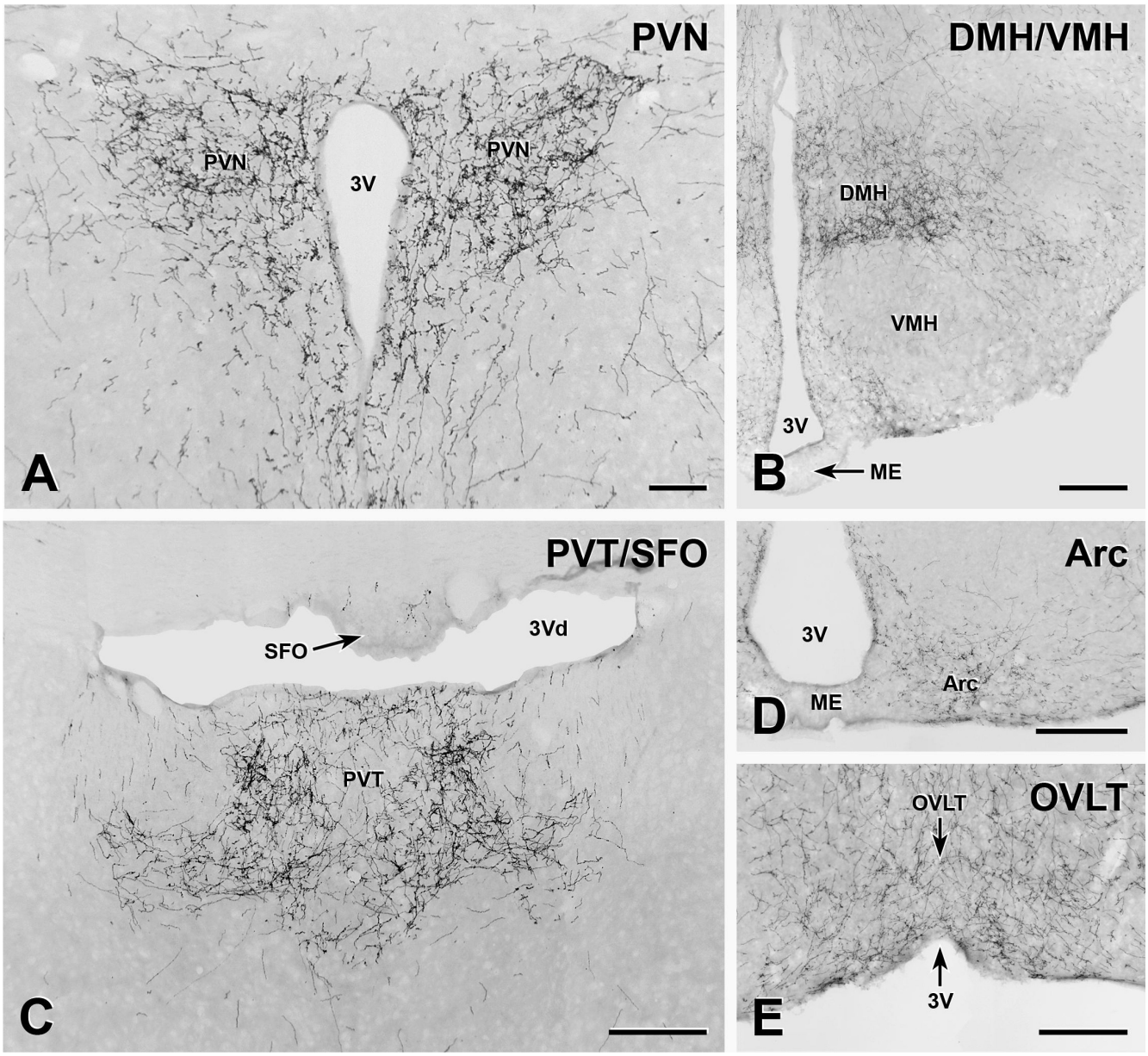

FIGURE 4. YFP-immunoreactive axons in hypothalamic and thalamic nuclei

A, The paraventricular nucleus of the hypothalamus (PVN) is densely innervated by YFP-immunoreactive axons. Bar, 100 μm. **B**, More caudally in the hypothalamus, the dorsomedial nucleus of the hypothalamus (DMH) receives dense supply of YFP-immunoreactive axons and the arcuate nucleus is moderately innervated. There are very few YFP-containing axons in the ventromedial hypothalamic nucleus (VMH) and the median eminence (ME) is free of innervation. Bar, 250 μm. **C,** YFP-immunoreactive axon heavily innervate the paraventricular nucleus of the thalamus (PVT). Occasional axons also occur in the subfornical organ (SFO). Bar, 250 μm. **D**, There is a moderate innervation of the arcuate nucleus (Arc) and no axons in the median eminence (ME). Bar, 250 μm. **E**, The organum

vasculosum of the lamina terminalis (OVLT) contains a substantial number of YFP-immunoreactive axons. Bar, 250 μm. 3V, 3rd ventricle; 3Vd, dorsal 3rd ventricle.

Europe PMC Funders Author Manuscripts

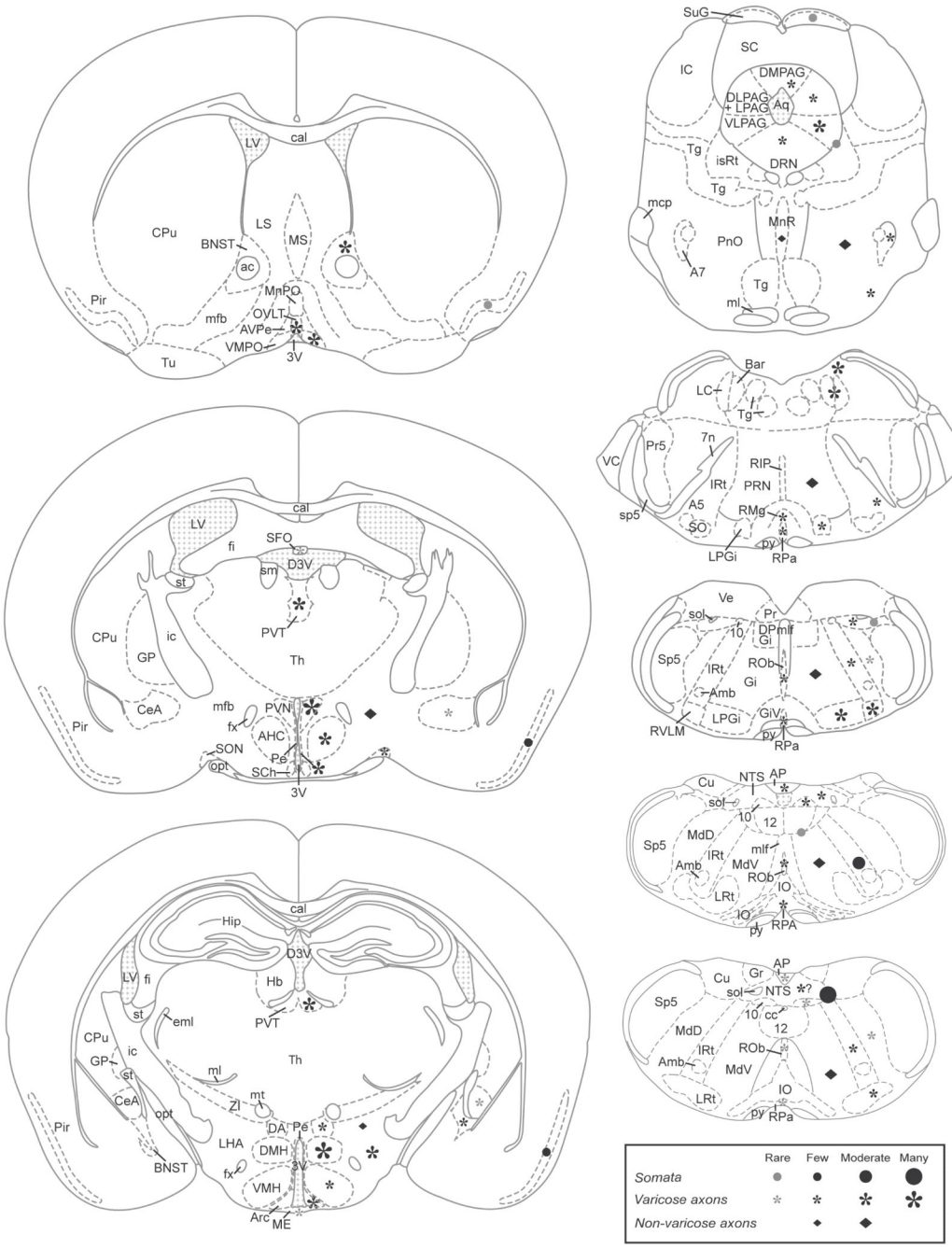

FIGURE 5. Distribution of YFP-immunoreactive cell bodies and axons in the brains of YFP-PPG mice

Diagrams of coronal sections showing the distribution of YFP-immunoreactive cell bodies and axons in the brains of YFP-PPG mice. Mapped sections were located between the spinomedullary junction and the rostral end of the third ventricle and were matched as closely as possible to the locations of the micrographs shown in Figures 1-4. Filled circles, YFP-immunoreactive somata; asterisks, varicose YFP-immunoreactive axons; diamonds, non-varicose YFP-immunoreactive axons. For all symbols, the size of the symbol indicates the relative density of the YFP-positive structure. Grey symbols indicate that the

immunoreactive structure is rare in that location. Although varicose, YFP-immunoreactive axons are present in the caudal NTS, it was difficult to assess their density because of the extensive network of YFP-positive dendrites that occurred in this region. Abbreviations: 10, dorsal motor nucleus of the vagus; 12, hypoglossal nucleus; 3V, third ventricle; 4V, fourth ventricle; 7n, facial nerve; A5, A5 noradrenaline neurons; A7, A7 noradrenaline neurons; ac, anterior commissure; AHC, anterior hypothalamic area, central part; Amb, nucleus ambiguus; AP, area postrema; Aq, aqueduct; Arc, arcuate nucleus; AVPe, anteroventral periventricular nucleus; Bar, Barrington's nucleus; BNST, bed nucleus of the stria terminalis; cal, corpus callosum; cc, central canal; CeA, central nucleus of the amygdala; CPu, caudate putamen; Cu, cuneate nucleus; D3V, dorsal third ventricle; DA, dorsal hypothalamic area; DLPAG, dorsolateral periaqueductal gray; DMH, dorsomedial hypothalamic nucleus; DMPAG, dorsomedial periaqueductal gray; DPGi, dorsal paragigantocellular nucleus; DRN, dorsal raphé nuclei; eml, external medullary lamina; fi, fimbria of the hippocampus; fx, fornix; Gi, gigantocellular reticular nucleus; GiV, gigantocellular reticular nucleus, ventral part; GP, globus pallidus; Gr, gracile nucleus; Hb, habenula; Hip, hippocampus; ic, internal capsule; IO, inferior olive; IRt, intermediate reticular nucleus; isRt, isthmic reticular formation; LC, locus coeruleus; LHA, lateral hypothalamic area; LPAG, lateral periaqueductal gray; LPGi, lateral paragigantocellular nucleus; LRt, lateral reticular nucleus; LS, lateral septum; LV, lateral ventricle; mcp, middle cerebellar peduncle; MdD, medullary reticular nucleus, dorsal part; MdV, medullary reticular nucleus, ventral part; ME, median eminence; mfb, medial forebrain bundle; ml, medial lemniscus; mlf, medial longitudinal fasciculus; MnPO, median preoptic nucleus; MnR, median raphé nucleus; MS, medial septal nucleus; mt, mammillothalamic tract; NTS, nucleus of the solitary tract; opt, optic tract; OVLT, organum vasculosum of the lamina terminalis; Pe, periventricular hypothalamic nucleus; Pir, piriform cortex; PnO, pontine reticular nucleus, oral part; Pr, prepositus nucleus; Pr5, principal sensory trigeminal nucleus; PRN, pontine reticular nucleus; PVN, paraventricular hypothalamic nucleus; PVT, paraventricular thalamic nucleus; py, pyramidal tract; RIP, raphé interpositus nucleus; RMg, raphé magnus nucleus; ROb, raphé obscurus nucleus; RPA, raphé pallidus nucleus; RVLM, rostral ventrolateral medulla; SC, superior colliculus; SCh, suprachiasmatic nucleus; SFO, subfornical organ; sm, stria medullaris; SO superior olive; sol, solitary tract; SON, supraoptic nucleus; sp5, spinal trigeminal tract; Sp5, spinal trigeminal nucleus; st, stria terminalis; SuG, superficial gray layer of the superior colliculus; Tg, tegmental nuclei; Tu, olfactory tubercle; VC, ventral cochlear nucleus; VLPAG, ventrolateral periaqueductal gray; VMH, ventromedial hypothalamic nucleus; VMPO, ventromedial preoptic nucleus; ZI, zona incerta. Diagrams have been reproduced from Franklin & Paxinos (2007), with kind permission.